

# The structural performance of arches made of few voussoirs with dry-joints

Ernest Bernat-Maso, Lluís Gil\* and Jordi Marcé-Nogué

*Department of Strength of Materials and Engineering Structures, Universitat Politècnica de Catalunya,  
Barcelona-Tech., ETSEIAT Campus Terrassa, c/Colom, 11, 08222 Terrassa, Spain*

*(Received January 11, 2012, Revised October 11, 2012, Accepted November 8, 2012)*

**Abstract.** This work approaches the structural performance of masonry arches that have a small ratio between number of voussoirs and span length. The aim of this research is to compare and validate three different methods of analysis (funicular limit analysis F.L.A., kinematic limit analysis K.L.A. and plane stress Finite Element Analysis F.E.A.) with an experimental campaign. 18 failure tests with arches of different shapes and boundary conditions have been performed. The basic failure mechanism was the formation of enough hinges in the geometry. Nevertheless, in few cases, sliding between voussoirs also played a relevant influence. Moreover, few arches didn't reach the collapse. The FLA and KLA didn't find a solution close to the experimental values for some of the tests. The low number of voussoirs and joints become a drawback for an agreement between kinematic mechanism, equilibrium of forces and geometry constraints. FLA finds a lower bound whereas KLA finds an upper bound of the ultimate load of the arch. FEA is the most reliable and robust method and it can reproduce most of the mechanism and ultimate loads. However, special care is required in the definition of boundary conditions for FEA analysis. Scientific justification of the more suitability of numerical methods in front of classic methods at calculating arches with a few voussoirs is the main original contribution of the paper.

**Keywords:** dry-joint arches; collapsing mechanism; experimental testing; FEA simulation; funicular analysis; kinematic analysis

---

## 1. Introduction

Masonry is the most common material in architectural heritage. It is made of bricks or stones that cannot bear tension and, in some cases, mortar joints whose tensile strength is almost negligible. It is rather impossible to build a bending beam using long masonry elements; nevertheless ancient builders gently overcome this limitation when built lintels of doors and windows with an arch shape in order to keep all arch's voussoirs always compressed. There are a lot of arch shapes and we limited our study to small semi-circular arches, like the Romanesque ones. This small span arches are composed with a limited number of voussoirs. Therefore, the ratio between the number of voussoirs and the height over the span length value is small, say  $Q < 50$  (Eq. (1)) for semi-circular arches. A lot of cracks in heritage buildings born and/or die in these arches because of the openings at façades and walls. For this reason, it is important to understand the structural behaviour of these

---

\*Corresponding author, Ph.D., E-mail: [lluis.gil@upc.edu](mailto:lluis.gil@upc.edu)

arches to prevent future pathologies during restoration works. What is more, the structural analysis of lintel arches is essential to proceed with a proper strengthening intervention and to ensure the proper safety factor of the design.

$$Q = \frac{\text{number of voussoirs}}{\text{height/free span}} \quad (1)$$

There are a lot of methods for the calculation of arches: some analytical methods are based on equilibrium (Audenaert 2007), while others uses kinematics (Chen 2007), numerical methods for funicular analysis (Andreu 2007), two-dimensional Finite Element Analysis (FEA) (Cavicchi 2006) or three-dimensional models (Fanning 2001). Some of them have been extended for vaults calculation (Milani 2008). Moreover, some finite element models use contacts (Drosopoulos 2006, 2008). Analytical and numerical methods for the calculation of masonry arches are based on the hypothesis that an arch is, basically, a continuum medium where geometrical discontinuities are rarely defined. Despite this simplification, these methods work successfully when calculating large structures, like bridges or cathedrals. For this kind of structures, obviously most challenging compared to lintels and far more studied, the ratio between the number of voussoirs and the height/span of the arches is tremendously high. Thus, the continuity hypothesis is almost true because the distance between joints is negligible compared with the structure size. Other geometric variables influences, like the shape of the arches, have been analysed by other authors (de Arteaga 2012).

Unfortunately, some of these calculation methods are limited when trying to predict the ultimate load of arches with a low ratio between the number of voussoirs and the height/span. Although none of them fully satisfy the geometrical constraint that represents to have very few voussoirs, no more research has been found in bibliography to justify using other methods either investigations proving better options for this specific case study. Furthermore, any model proposed to calculate these structures should be experimentally validated. In order to analyse this structural problem and to provide a scientific basis for the use of FEA in arches with a few voussoirs, 18 experimental tests on dry-joints masonry arches were carried out. Their results were compared with the ones obtained from two classic calculation methods: an analytical calculus method based on the kinematics of the failure (kinematic limit analysis, see Chen 2006) and an equilibrium based numerical method (limit analysis with elastic catenaries elements, see Andreu 2007). Experimental results were also compared with an up-to-date Finite Element Method (FEM) micromodel performed with a commercial FEA package (ANSYS® v.12.1).

The research finished with a few highlights related with the suitability of some classic calculation methods (KLA and FLA) at solving the structural problem of an arch with little number of voussoirs. Finally, particularities that should be taken into account using FEA at solving this problem are provided when presenting a fully operational numerical model which accurately represents the laboratory tests.

## 2. Test configuration and procedure

Experimental tests on masonry structures are always complex. First of all, tests tend to provide scattered results (Boothby 2001). Secondly, and especially in the studied case of dry-joint voussoirs, arches construction easily drives towards geometries that contain initial imperfections that might affect dramatically the results (de Arteaga 2012). Finally, the load application may lead to undesired

mixed failure mechanisms that difficult the interpretation of the experimental tests. Strengthening systems tend to uniform the response of masonry arches and this is one reason because most of the recent experiments have been carried out on strengthened specimens (Borri 2011 or Garmendia 2011) although there is not yet a full understanding on the behaviour of non-strengthened masonry arches with a small ratio between number of voussoirs and height/span ratio.

The experimental campaign was designed and executed assuming several limitations. 18 dry-jointed arches were built and loaded until collapse with 6 different geometry shapes (see Fig. 1 and Table 1). Voussoirs were produced by pouring fresh mortar in a mould. The material of the voussoirs is a poor portland cement mortar. All arches were 152 mm width (out-of-plane size) and 100 mm thickness. The size of the specimens was chosen to fit with common real lintel arches over doors

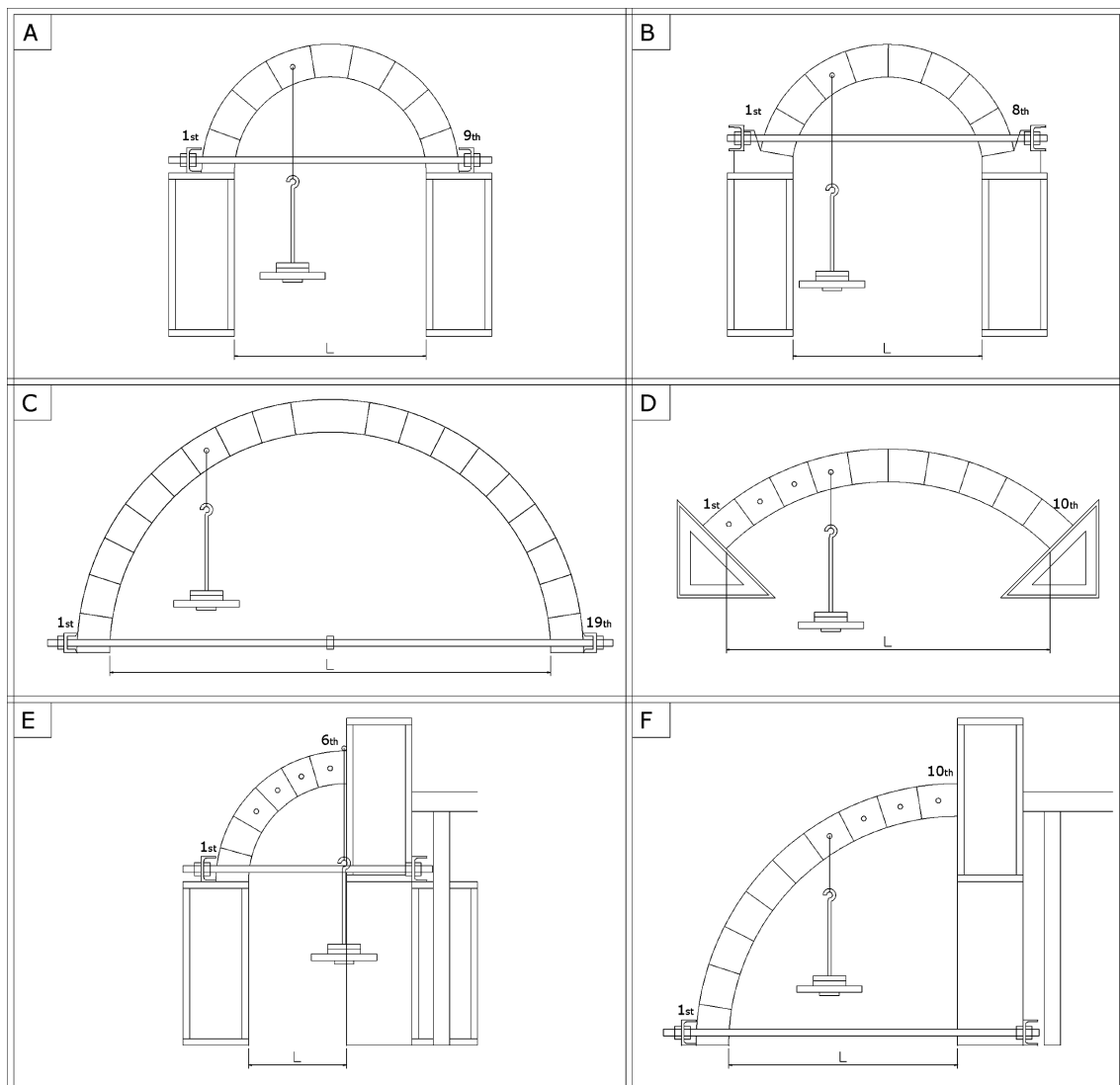


Fig. 1 Tests setups

Table 1 Geometry of the tested semi-circular arches

Arch	Test	Number of voussoirs	Free span L (cm)	Loaded voussoir	Self-weight (N/m <sup>3</sup> )
A	A.1.1	9	59.5	4th	19104
	A.2.1		58.7		
B	B.1.1	8	58.0	3rd	19104
	B.1.2		58.0		
	B.2.1		58.2		
C	C.1.1	19	134.9	7th	18134
	C.1.2				
D	D.1.1	10	97.6	3th	18134
	D.1.2				
	D.1.3				
E	E.1.1	6	30.1	4th	20158
	E.2.1		30.1	5th	
	E.3.1		30.2	6th	
	E.4.1		30.1	*	
	E.5.1		30.6	*	
	E.6.1		29.4	*	
F	F.1.1	10	69.0	7th	18134
	F.2.1			9th	

\*Loaded near to the end at extrados (see Fig. 1 part E)

Table 2 Mechanical properties of the mortar used to build the arches

Arches	Self-weight (N/m <sup>3</sup> )	Compressive strength (MPa)	Young's modulus (MPa)
A/B	19104	4.76 [0.52]	84.06 [41.89]
C / D / F	18134	1.26 [0.11]	78.19 [40.79]
E	20158	3.03 [0.57]	79.75 [35.47]

and windows.

The load was applied step by step, being always in a perfect vertical alignment. The position of the load for each test is summarized in Table 1. An auxiliary metallic structure restrained the horizontal displacements at the supports of arches, see Fig. 1.

Table 2 summarizes the mechanical properties of the mortar used for each arch. All values were experimentally obtained. The coefficient of variation of the compressive strength and the Young's modulus is included in brackets next to the experimental values. Nevertheless, these properties are not so much important in this study because the collapse of the structure is a geometrical instability process caused by the formation of 4 hinges in most of the cases. There were no tensile cracks observed neither compression-caused damage appeared in voussoirs for compressive stresses. Any

experimental collapse was related with the material strength. As it can be found in related scientific literature (e.g., Heyman 1997), the stress level in dry-jointed arches is usually very low. Hence the failure is a matter of pure geometry and material strength is less relevant. However, material deformability properties play a leading role as they define how the geometry of the structure varies during the test.

### 3. Test results

All 18 tested arches were dry-joint masonry arches. The material of the voussoirs was portland cement mortar. Every experimental test carried out is identified in the second column of Table 3 by a letter that refers to the shape of the arch tested (see Fig. 1) and two numbers. The first one refers to the case tested (geometry little variation and/or loading) and the second value represents the repetition number of the same test. Only tests B1, C1 and D1 were repeated.

Two different types of collapse were observed in the experimental campaign. The first one is the failure mechanism that happens when at least 4 hinges at alternated sides of the arch appear. Most voussoirs kept full surface contact with the neighbour voussoirs whereas some joints opened generating natural “cracks”. In these last cases, voussoirs kept in contact in a small line that became an axis of relative rotation. This axis can be settled at the intrados or at the extrados (see Fig. 2). The second kind of collapse was caused by relative sliding between neighbour voussoirs. The contact between voussoirs did not develop enough friction to prevent the relative glide of voussoirs. This happens because the arches were “too” light-weighted and they do not produce a relevant normal force at the contact surface due to the self-weight. Therefore, in spite of the proper roughness of the mortar surface, the structure could not stop the relative glide. Third and fourth column of Table 3 show the test results, with the load-bearing capacity of each arch and the observed failure mechanism: hinges mechanism (M) or combination of hinges mechanism and sliding (M + S). Notice that experimental load-bearing capacity is an upper limit and the real failure load could be a few lower. This is because the load was applied step by step and the recorded result is the last load that produces the collapse.

Finally, another group of arches did not fail. Tests E.1.1, E.2.1 and E.3.1 bore the maximum load that we could apply with the loading system: 546 N.



Fig. 2 Collapse mechanism of test B.2

Table 3 Results summary

Arch	Test	Collapse load (N)	Mode of failure**	Funicular analysis Ultimate load (N)	Kinematic limit analysis Ultimate load (N)	Finite element method (FEM) Ultimate load (N)
A	A.1.1	326	M	250	495	331
	A.2.1	301	M	253	511	343
B	B.1.1	335	M	450	750	295
	B.1.2	276	M	450	750	295
	B.2.1	301	M	470	745	294
C	C.1.1	95	M+S	90	435	102
	C.1.2	90	M	90	435	102
D	D.1.1	423	M	550	1657	407
	D.1.2	350	M	550	1657	407
	D.1.3	521	M+S	550	1657	407
E	E.1.1	No collapse	-	-	-	7795
	E.2.1	No collapse	-	-	-	938
	E.3.1	No collapse	-	2200	-	458
	*E.4.1	206	M	275	274	194
	*E.5.1	196	M	240	251	183
	*E.6.1	221	M	325	315	211
F	F.1.1	275	M	500	2506	323
	F.2.1	49	M+S	43	284	47

\* Loaded near the arch ending at extrados (see Fig. 1 part E)

\*\* M means mechanism formation (4 hinges) and S means sliding failure mode

In order to deeply analyse the results it is highly recommendable to look at the description of the experimental observations summarised in the Annex.

Comparison of behaviour of tests A.1.1 and A.2.1 points out the noticeable influence of the initial geometry in these types of tests. Having an initial joint opened in the position where it is finally placed at failure contributes to change the order of hinges' opening.

Comparing the behaviour of tests of arches B, it is noticeable that having or not having joints initially opened influences a lot the deformational response of the arch. Whilst tests B.1.2 and B.1.2, both with hinge H4 initially opened, showed great deformations before failure, for test B.2.1, with all joints closed, the deformation at collapse point was hardly noticeable. Differences between tests B.1.1 and B.1.2 might be caused by geometric imperfections due to the manual mounting system of the arches.

As the initial conditions were the same the ultimate response of arches C.1.1 and C.1.2 was analogue. The only difference observed was the presence of the sliding process in test C.1.1. However, the maximum load as well as the qualitatively observed deformation were equivalent which could indicate that the sliding may be a consequence of the dynamic movement when falling.

Comparing tests D it is clearly proved there is a relationship between the position of the hinges (failure mechanism shape), the order they appear and the maximum load the arch can bear. It experimentally proves the scientific basis of kinematic limit analysis. Developing one or another mechanism may depend on little initial geometric differences but the sensibility seems noticeable. The early opening of the extreme hinge allowed the sliding of the left extreme of the D.1.3 arch modifying the shape which became more flat. Thus, it influenced the results increasing its load-bearing capacity.

From tests E.1.1, E.2.1 and E.3.1 the results showed that the arches' shape related with the load application point made it possible to transfer the load to the supports directly so the failure mechanism was not developed. However it is worth mentioning the noticeable deformation observed during these tests which indicates that the Young's modulus of the voussoirs may be an essential variable to correctly study the arches behaviour when the stress level is high. Comparing E.4.1, E.5.1 and E.6.1 no discussion may be done except from remarking the influence of the span length and the initial geometry in the behaviour of this type of arch formed by a few voussoirs. The load bearing capacity seems to decrease when increasing the span. This behaviour contradicts the theory and the observations made for tests on arches A. This contradictory response may be caused, in this particular case, because increasing the span may mean having initial contacts more opened instead of getting a flatter arch.

Comparing the two tests of F series, the influence of the load position is clearly observed. They represent half an arch, so if the load is centred in a full arch (case to be represented by test F.2.1), the loadbearing capacity is bigger than if the load is closer to  $\frac{1}{4}$  of the span (case represented by test F.1.1).

#### **4. Funicular limit analysis (FLA)**

It is well known that Robert Hooke said that the ideal shape of a masonry arch in equilibrium with certain loads is that of the inverted catenaries curve drawn by a chain subjected to the same weights (Heyman 1997). The possibility of analysing masonry arches by means of the analogy between the equilibrium of compressed members with that of funicular models only working in tension has been used for the assessment of important constructions (f.e. Poleni in the case of the dome of St. Peter in the Vatican, or Gaudí to design very complex structures based on 3D hanging models such as the Church of Colònia Güell). The hanging catenary is equivalent (drawn up side down) to the thrust line of the arch and it has to fit inside the boundary of the arch to be able to assure that the arch is stable and full fills equilibrium.

Heyman's formulation for the plastic (or limit) analysis of masonry arches (Heyman 1997) provides a theoretical and comprehensive base for the analysis of this type of constructions. Limit theorems of plasticity are applied to masonry structures provided that they verify the following conditions:

- a) Compression strength of the material can be considered infinite. This hypothesis is based on the fact that stresses in masonry are normally very low in relation to its ultimate load capacity. Consequently, structural failure is rarely reached due to crushing of the materials in compression.
- b) Collapse due to the sliding between parts is impossible. This hypothesis assumes that friction between the voussoirs is high enough to prevent sliding between them. It is not always true and

sliding collapses may occur in flat arches or light arches.

- c) Tensile strength of masonry is negligible. This approach is exact in the case of the studied dry-joint masonry and sets calculations in the safe side in the case of mortar joints.

Under these hypotheses, it is proved (Heyman 1997) that the arch is structurally safe if there is a thrust line that can be drawn inside the arch boundaries. This procedure finds a lower limit of the load-bearing capacity of the arch. Andreu proposed a computational elastic catenary element that conserves the unit weight after deformation, see details and a full description at Andreu (2007). This

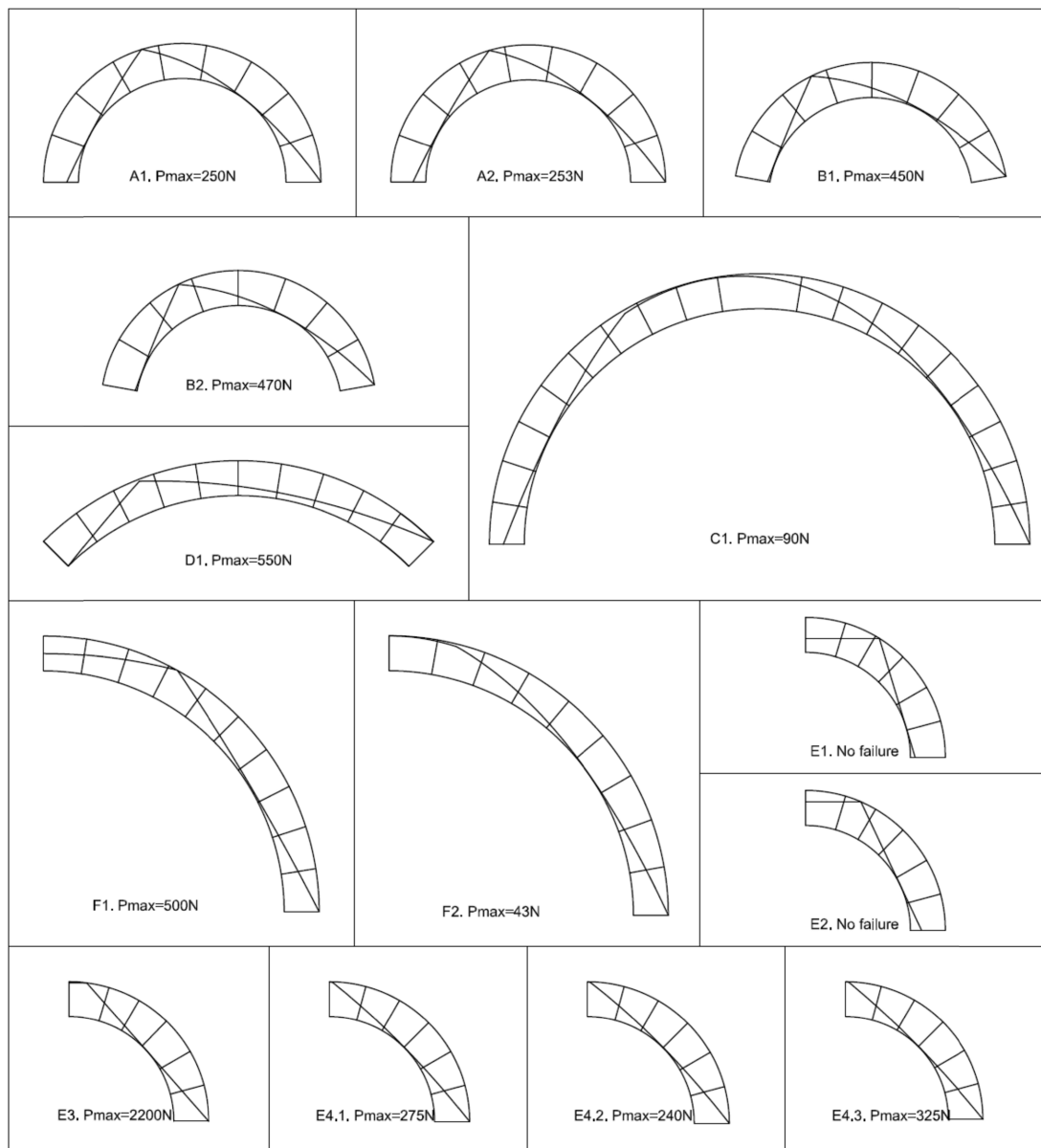


Fig. 3 Thrust line calculated for each tested arch

approach has been used to calculate the shape of catenaries. Results of the calculus carried out with this method are shown in Table 3. Thrust lines calculated are presented in Fig. 3.

The procedure consisted in calculating the deformed shape of an elastic catenary element suspended from two points placed at a fixed distance equal to the existing gap between two points where the thrust line pass by in the real arched structure near the failure time. This means the distance between two points close to the boundary of the arch and coinciding with joint section. The elastic catenary element was loaded with the same loads than the real arch. It is the self-weight, distributed along the catenary, and the punctual load which was maintained always vertically aligned with its initial position to respect the test setup and execution. Once the shape of the catenary was calculated it is drawn upside down inside the arch geometric boundary (see Fig. 3). If the catenary is inside the boundaries the arch is safely stable under the applied load. Bigger load was then tested and the process was repeated to optimise the obtained solution (increase the applied load while maintaining the catenary or thrust line inside the boundaries of the arch). For detailed procedure or full mathematical description of the model, see Andreu (2007).

Maintaining the catenary inside the arch assures no tensile stresses were developed (safety criteria of the lower limit theorem), keeping the vertical alignment of the load is intended to represent the real test conditions and adjusting the catenary to pass closer to the arch's boundaries at four points coincident with real joints between voussoirs is to respect the kinematic conditions of the problem. According with the theory (Heyman 1997) a hinge will appear at each point the thrust line pass tangent with the arch's boundary and as long as hinges in real tests may only appear in real joint positions, respecting this criterion is equivalent to respect the kinematic compatibility between arch's parts and leads to obtain the real maximum load that may be applied on the arch. In the application of FLA in the present research this last condition was not fulfilled (see the graphic results of A1, A2, B1, B2, D1, E2 in Fig. 3) and a lower limit of the load bearing capacity was obtained. It is equivalent to the consideration of extra friction interfaces in the analysis.

To obtain a more flexible calculus method, this same procedure was tentatively used with the follow modifications:

- Allowing the thrust line going outside the boundaries as some tensile strength may be attributed to the voussoirs material. This option was limited to going outside and returning inside at the same voussoir because the real joint may not bear any tensile stress. Some applications of this method have been proved effective in structures with far more voussoirs. See Roca (2006). However, defining the extra gap the thrust line is allowed to separate from the arch boundary is complex (see Roca 2006). Most of the time the limitation is that the thrust line could not stay outside the boundary for two or more adjacent voussoirs. This method has proved to be unsafe in some cases. e.g. for arch A.1.1 the maximum load calculated this way was 360 N. Fig. 4 shows the shape of the catenary corresponding with this calculus, limiting the catenary position by the requirement of do not stay outside for two or more consecutive voussoirs.
- Allowing the thrust line to move horizontally to adjust better the tangency point with the boundary with the real joints position. This procedure was in conflict with real test setup and with the hypothesis that the original shape is valid to carry out this calculus. Results calculating arch A.1.1 this way are graphically presented in Fig. 5. Results are too conservative: 285 N in front of the 326 N experimentally obtained. However, this procedure does not have a solid basis as it changes the real load position.

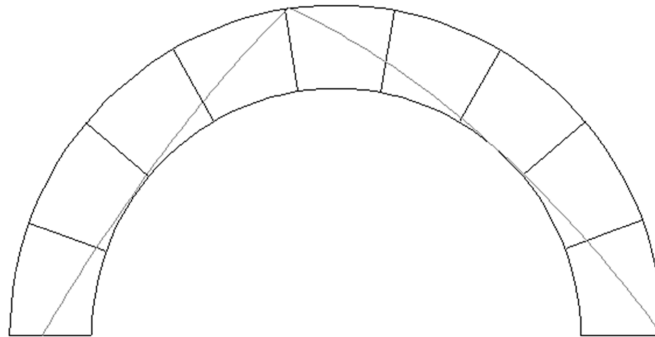


Fig. 4 Thrust line calculated without keeping the vertical position of the load. Arch A.1.1

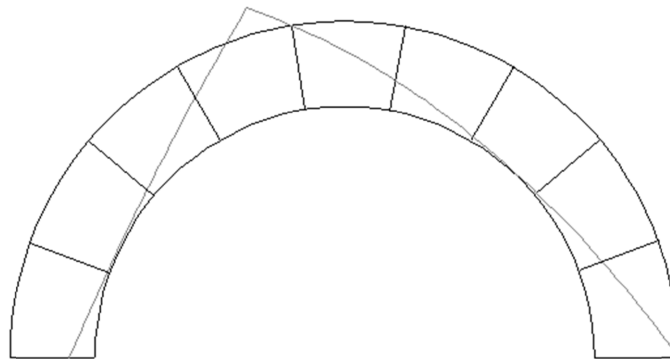


Fig. 5 Thrust line allowed overpassing the arch boundaries. Arch A.1.1

## 5. Kinematic limit analysis (KLA)

Kinematic limit analysis is a classical calculus method widely used. It is based on guessing a compatible mechanism for the collapse mode, and according with this mechanism, imposing the equilibrium of the energy associated with the external loads. Generally on arches calculus, it is assumed that energy associated with the internal strains and stresses of the structure is negligible in front of the energy required to move the structure up to the collapse.

The procedure (Chen 2006) consists on dividing the arch in four pieces. Three of them rotate respect a centre of rotation geometrically determined or imposed at guessing the mechanism shape. As self-weight and applied vertical punctual load are the only external loads considered in the calculus, there is only interest on considering the vertical displacements of the gravity centre of each piece of the arch and the vertical displacement of the point where the punctual load was applied. A relationship between these vertical displacements can be geometrically determined. From the imposed energy equilibrium equation, a value for the punctual load can be then obtained. Arches E and F were considered as complete arches with symmetric loads and boundary conditions (see Fig. 6). Calculations were done by drawing (with computer aided drawing software) the rotation of different parts of the arches. These rotations were geometrically related. The energy needed to move the arch in failure was calculated multiplying the self-weight of each voussoir by the

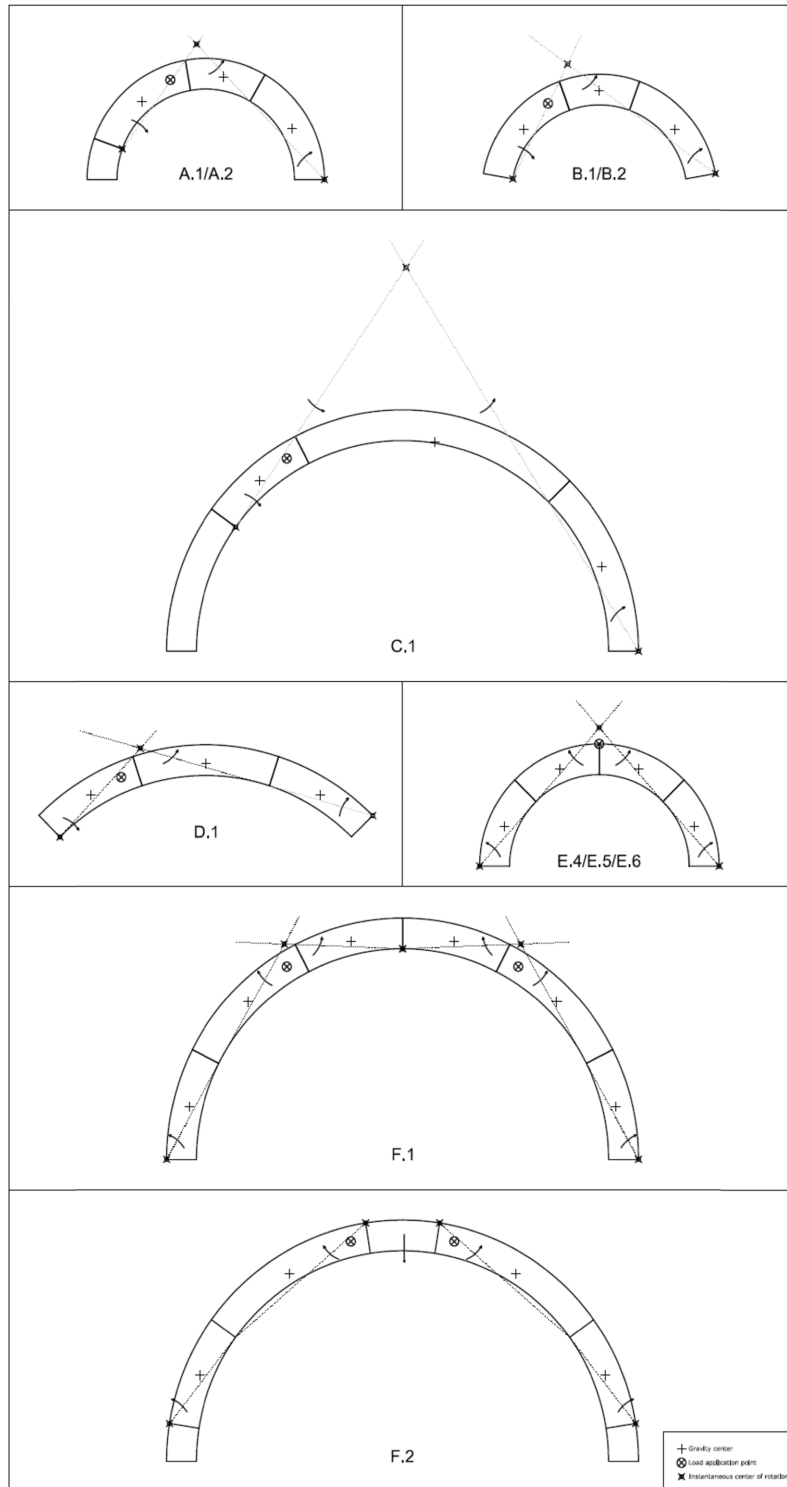


Fig. 6 Mechanism for kinematic analysis of each tested arch

vertical component of the displacement of its centre of gravity. Adding all quantities plus the applied vertical punctual force by the displacement of the application point, zero-balance energy should be obtained. To meet this requirement, the punctual load value was manually calculated. To more detailed information about this calculus method and possible implementations, the reader is referred to Chen (2006).

This process could be repeated for every possible mechanism. However, the better accuracy corresponded with using the experimentally observed failure mechanisms. For this reason the real failure mechanisms (see Fig. 6) were used in the present research.

It is well known that KLA method provides an upper limit for the failure load of the structures. For all tested arches, the guessed mechanism for the calculus was the one closest to the experimental failure shape observed. Using extra virtual or fictitious joints in the calculus may provide more accurate results but it required the crack of the voussoirs (reaching the tensile strength of the mortar) to base this procedure. As long as any of the voussoirs cracked during the tests, it was preferred to stick to the real discretisation of the arch and the observed failure mechanism.

Results of the calculus carried out with this method are summarized in Table 3. Each guessed mechanism is shown in Fig. 6.

## **6. Finite element analysis (FEA)**

We selected ANSYS® v.12.1 for Windows XP (32-bit system) to carry out the analysis with the aim of using general purpose FEA software widely spread among practitioners. The main features of the models implemented regarding materials definition, geometry modelling, contacts definition, boundary conditions, loading method and results analysis are described below.

The problem type was two-dimensional plane stress (depth = 152 mm) with large deflections. The geometry of each arch was created with Computer Aided Design software such AutoCAD® and consisted in several bodies in contact. Each body represents one real voussoir of the dry-jointed arches.

To represent more realistic supports, a rectangular piece of steel was defined in the simulation at the feet of the arch. The piece was fully displacement restrained at the bottom side. The problem involves different materials and surfaces in contact. The non-linear material response and the accurately contact definition are a challenge. Firstly, the dry joints of the arch require the simulation of the contact between voussoirs and between voussoirs and supports. Two bodies are in contact when two separate surfaces of each body touch each other in such a way that they become mutually tangential. The dry-joint contact between voussoirs was performed with a contact model called cohesive zone (CZM) model that allowed an initial tensile and tangential strengths (Alfano 2001). When stresses exceed these strengths the contact allows the relative displacements between the bodies initially bonded. To represent the case of dry-jointed arches, CZM needs a fictitious tensile stress, shear stress and fracture energy; all of them were values close to zero.

On the other hand, the contact between the voussoirs and the steel supports was defined as Bonded, Frictionless, Frictional or Rough depending on the type of test performed. The Bonded contact assumes no gaps and no friction between the bodies which keep always stacked. The Frictionless contact assumes that a gap is allowed in the normal direction and sliding is allowed in the tangential direction. Frictional contact assumes the gap but sliding is not freely allowed. This model defines an equivalent shear stress at which sliding on the geometry begins as a fraction of the contact pressure

Table 4 Arch-support contacts definition in FEM simulation

Arch	Test	Model	Left support contact*	Right support contact*
A	A.1.1	A1	Rough	Rough
	A.2.1	A2	Rough	Rough
B	B.1.1	B1	Frictional 0.45	Frictional 0.45
	B.1.2			
	B.2.1	B2	Frictional 0.45	Frictional 0.45
C	C.1.1	C	Rough	Rough
	C.1.2			
D	D.1.1	D	Frictional 0.25	Frictional 0.25
	D.1.2			
	D.1.3			
E	E.1.1	E1	Rough	Frictionless
	E.2.1	E2	Rough	Frictionless
	E.3.1	E3	Rough	Frictionless
	E.4.1	E4a	Rough	Frictionless
	E.5.1	E4b	Rough	Frictionless
	E.6.1	E4c	Rough	Frictionless
F	F.1.1	F1	Rough	Frictionless
	F.2.1	F2	Rough	Frictionless

\*According with drawing on Fig. 5

defined by a friction coefficient. The friction coefficient (experimentally determined and summarised in Table 4) changes its value according the slope of the contact and the materials in contact. Once the shear stress is exceeded, the two geometries will slide relative to each other. The Rough contact is used when the friction coefficient between the contacting bodies is infinite, so the gap is allowed but the sliding is not.

In the gap direction, a pure penalty-based contact formulation with large Normal Stiffness and auto-asymmetric behaviour are assumed in which only the contact surfaces are constrained from penetrating the target surfaces (Eq. (2))

$$F_{normal} = k_{normal}x_{penetration} \quad (2)$$

When the sliding is not allowed, the two bodies should not slide relative to each other. For the tangential direction, pure penalty formulation is always used (Eq. (3))

$$F_{tan\ gential} = k_{tan\ gential}x_{sliding} \quad (3)$$

These formulations imply a non-linear solution. A convergence iterative procedure based on a

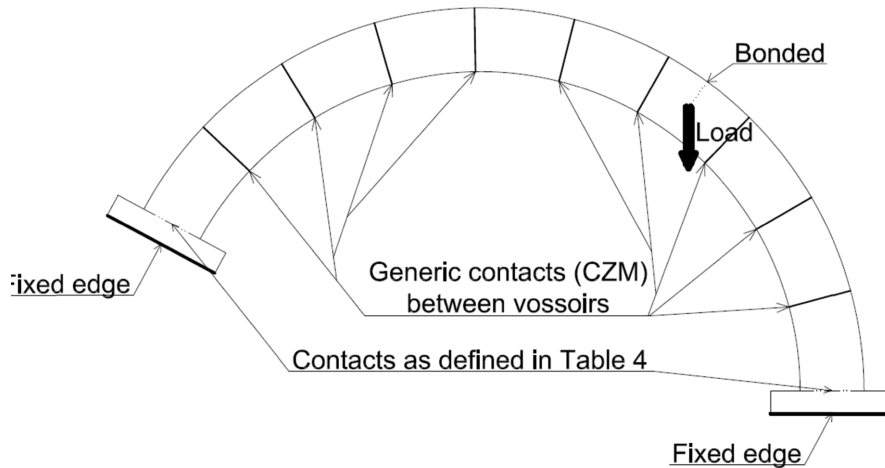


Fig. 7 Boundary conditions and contacts definition in FEA

Newton-Rhapson iterative algorithm was used. Fig. 7 shows the different type of contacts and boundary conditions while Table 4 summarizes all of them for each geometry.

Instead of applying a load at the centre of the loading vossoir (see Fig. 1) like it was done in the experimental test, a descending displacement over the loading point was imposed and the force reaction was recorded and assumed as the bearing capacity of the arch.

The solve procedure and the mesh generation are performed by using the automatic algorithms available in the FEA package by default. The mesh used quadrilateral elements with an average length of the edge of 5 mm. Below this size no variations on the results were noticed so this size was fixed as the one to be used in the simulations.

Regarding the material, it is worth mentioning that all experimental arches were dry-joint arches with mortar vossoirs. This material (mortar) was defined as a perfect plastic material with Young modulus of 80 MPa, Poisson ratio of 0.40 and ultimate compressive stress of 3 MPa. It is a simplification of the material behaviour that has proved easy and accurate in these simulations. The compression strength (3 MPa) and Young's modulus (80 MPa) are the average values of all tests on the mortar used to produce the vossoirs. Observing the values in Table 2 it is noticed that the scattering of these two parameters was so high, especially for the Young's modulus, that it made no sense to distinguish between arches typologies. Moreover, the compressive strength has low significance in the simulations as the arches failed by the formation of the mechanism and never crushing the material. However, the greater the Young's modulus is, the stiffer the structure would behave and more stress concentrations would appear. In this case, the compressive strength would be an important parameter to take into account if analysing arches with high Young's modulus for which the crushing of the material was a real failure possibility. Having said that and given the Young's modulus was more or less the same for all the mortar used to produce vossoirs, using averaged parameters of compressive strength and Young's modulus was consistent.

It should be observed that the possibility to develop a mechanism from an initial stable over constrained structure needs the structure to deform and modify its shape in order to make it possible the formation of the hinges. This behaviour significantly depends on the value of the Young's modulus of the material the vossoirs are made of (poor cement mortar in the present research).

Table 5 Relative results errors respect the average experimental values

Arch	Test	Funicular analysis Relative error (%)	Kinematic limit analysis Relative error (%)	Finite element method (FEM) Relative error (%)
A	A.1	-23.3	51.9	1.4
	A.2	-15.9	69.8	14.0
B	B.1	47.3	145.5	-3.4
	B.2	56.1	147.5	-2.4
C	C.1	-2.7	370.3	10.0
D	D.1	27.5	284.2	-5.5
E	E.4	33.5	33.1	-5.9
	E.5	2204	28.0	-6.4
	E.6	4701	42.4	-4.5
F	F.1	81.8	811.3	17.4
	F.2	-12.2	479.0	-3.4
Average**		33.6	223.9	6.8

\*Only experimental tests which reach their ultimate strength are included.

\*\*Average of absolute value of relative errors respect the average experimental collapse load for each case.

Although doing a sensitivity analysis was not the aim of the present research, it was observed that varying the Young's modulus (E) from 40 MPa to 160 MPa the load bearing capacity of the arch A.1.1 varies from 232 N to 519 N. So the presented model is highly dependent on the value of E and correctly determining this variable is required to obtain accurate results.

Poisson value was set at 0.4. Variations in the results below the threshold value of 3% were obtained when varying Poisson's value from 0.25 to 0.45 for simulations of arch A.1.1.

Results of the simulations are summarised in Table 3. The average relative error was 6.8% (see Table 5). For cases of A and C series (complete semi-circular arches) the model tends to slightly overestimate the loadbearing capacity of the arches compared with experimental results. For these arches the compressive behaviour of the material had less importance in the simulation result as the mechanism is developed at relative low loads. In contrast, the model underestimate the capacity of arches from E series for which the frictionless contact with the vertical support could be too conservative. Comparing the results of the simulations of cases E.4.1, E.5.1, and E.6.1 as well as comparing F.1.1 and F.2.1, the influence of the position of the load is clearly reproduced by the model. The nearer the load application point is to the centre of a full arch, the greater its load bearing capacity is. As the geometry of tests of A, B, C and D series did not vary from one repetition to another or the changes are little, the results of the numerical model are constant within each series.

Stresses in the voussoirs are always little compared with the mortar strength. Only for case E.1.1 the stresses concentrated around the load application point were close to the maximum strength. However, in this case the simulated arch reached a compressive failure at loads far larger than the capacities of the experimental test setup, extending the range of applicability of the model far away from the experimental limits of the present research.

## 7. Discussion

In the last three columns of Table 3 are respectively presented the results of the funicular analysis, the kinematic limit analysis and the finite element method analysis described before. The first thing to notice is that FEA is the single method that provided always an ultimate load value whereas the other two methods fail when common hypothesis, as the ones presented above, are considered. When we performed a funicular analysis, it was observed that it is possible to draw two straight lines inside the arch for cases E.1.1 and E.2.1; and get equilibrium with the external load. According to the plastic theorems of Heyman (1997), this means that these two arches can bear any load without creating a mechanism; therefore the arch should only collapse by a sliding mode or by crushing the material. For this reason, there is no value in the cells of the table corresponding with the funicular analysis of cases E.1.1 and E.2.1.

On the other hand, when we performed a kinematic limit analysis for the cases E.1.1, E.2.1 and E.3.1 it was not possible to find a solution. Because of the geometry of the arches it was rather impossible to the authors to find a 4-hinged mechanism compatible with the boundary conditions and the imposed load (vertical, descending) at the same time. Assuming extra friction joints will make it possible to solve the problem but it would not be really representative of a real case as the hinges should develop only in real joints. No voussoir cracked by tensile forces. Any other joint opened apart from the existing ones between voussoirs.

Comparing the results of the funicular analysis and the kinematic limit analysis it is observed that the first one provides lower values for the load bearing capacity of the arches than the second one. Therefore the funicular analysis finds a lower bound of the ultimate load for linear masonry structures while the kinematic limit analysis finds an upper limit of the ultimate strength. Although this, it is not exactly true for two results, tests E.4.1 and E.6.1, in these two cases, both methods reach almost the same result, so it can be understood as the real collapse load.

From the comparison between the experimental results and the ones obtained from the funicular and the kinematic analysis, it seems clear that in cases A and C the experimental collapse load is inside the interval defined by the funicular calculus (lower bound) and the kinematic results (upper bound). For us, it is no merely a coincidence that these two arches (A and C) were the only ones that had both feet in a way that sliding was absolutely forbidden and the failure developed a full 4-hinges mechanism. We think that classic funicular and kinematic analysis always report a valid result when arches collapses with a pure 4-hinges failure mechanism; for all other cases this seems not to be necessarily true. If ever any sliding is allowed during tests, like cases B, D, E and F, then classic funicular analysis (expected lower bound) might provide ultimate loads higher than the experimental ones.

Comparing the experimental results of arches A and C (slight or no sliding effects) with the calculation using the funicular limit analysis (see Table 3); it was observed that if the thrust line touches the boundary in points near the real joints between voussoirs (C case), then the calculated ultimate load finds a value very close to the experimental one. However, if the thrust line becomes tangent to the boundary in the middle of a voussoir (A case) or quite far from the real joint, then the calculated results may differ very much from the experimental collapsing loads. As a rule of thumb, the less number of voussoirs have an arch, the more difficult is to draw a thrust line that reproduces the failure mechanism with hinges at the real joints and therefore the funicular analysis become less accurate. The same happens with the kinematic limit analysis because the less voussoirs, less real joints and it is more difficult to find a boundary-compatible mechanism of failure.



Fig. 8(a) Stress distribution for each FEM

Generally speaking, results obtained with funicular limit analysis do not match precisely with experimental ones. There is a geometrical reason for that. Firstly, hinges must develop at points where the thrust line is tangent to the arch boundary. For real mechanisms, hinges always develop at joints between voussoirs; nevertheless calculated thrust lines may not exactly fit hinges at real joints and hinges may theoretically appear, for example, in the middle of a voussoir. This situation is obviously in contradiction with the real collapse. Therefore, the first kinematic condition to full fill



Fig. 8(b) Stress distribution for each FEM

is to respect the real mechanism and force the geometry of the thrust line to fit with the real hinges. On the other hand, due to the punctual load, the vertex of the calculated thrust line has to be vertically aligned with the real loading point to full fill an equilibrium condition. When the thrust line is forced to fit the real mechanism, the vertex of the catenary is shifted and the equilibrium is lost; whereas when the vertex is correctly aligned and the equilibrium is full filled the hinges appear at points without a joint and the collapse mechanism is false. To sum it up, the prediction of the load bearing capacity using funicular limit analysis requires that the thrust line respects both: the real failure mechanism and the force equilibrium. These two simultaneous requirements are easy to achieve for arches that have a large number of voussoirs like bridges or cathedrals where arches have large spans. But when the arch is made of few voussoirs it is extremely difficult to respect both conditions at the same time.

All the simulations carried out with the presented FEA resulted in a mechanism or a composed mechanism-sliding failure mode, except the two corresponding with the cases E.1.1 and E.2.1 for which the collapse was associated with the material failure. Failure stress distribution is graphically summarized in Fig. 8 where it is also possible to notice that stresses are low as limit theories pointed out. This is the case for almost all the analysed arches.

Table 5 shows that the calculation method that better fits with the experimental results is the finite element analysis (FEA) presented with an average relative error of 6.8% in front of 33.6% by the funicular analysis and 223.9% by the kinematic analysis. FEA achieves a good accuracy both predicting the ultimate load and the mode of failure of most of the analysed arches. FEA has the possibility of take into account the boundary conditions (Table 4) in a more efficient way than the other two methods used in this paper which supposed that sliding is not allowed. For this reason, the results obtained with the FEA are closer to the experimental ones than the obtained with the funicular or the kinematic analysis.

The less accurate prediction of the FEA presented corresponds with the test F.1.1 and has a relative error of 17.4% respect the experimental value. Because of the heterogeneity of masonry and the great influence of the arches manufacturing process on their strength and deformability properties, this error is high but seems acceptable for a single case, more if the method (FEA) shows a very good capacity to predict the ultimate load of most of the tested arches. However, the dependency of the results of the FEA on the value of Young's modulus makes this model very sensible to this parameter which should be accurately determined.

## **8. Conclusions**

Masonry arches are very common for lintels of windows and doors. Because of the openings at façades and walls, lintels are points of crack localisation. Lintel arches are made of few voussoirs and this geometry constraint dramatically affects their structural performance compared to all large span arches. This study contains an experimental campaign of 18 arches made of few voussoirs with dry-joints and the comparison of the collapse mechanism with three calculation methods.

Firstly, notice that the failure mechanism of presented arches is different from large span arches. For large span arches the common failure mechanism is the relative rotation and the formation of enough hinges while sliding also happens but a few. In our experimental tests we identify both failure mechanisms. The failure of sliding happened because the weight of the arch was small and could not develop enough friction at joints. For real structures we expect that this rarely will happen

because the upper weight of the wall loads and stabilizes the arch. We want to point out that the collapsing mechanism for hinge formation is constrained by the geometry; hinges only can develop in a limited number of joints (few voussoirs) and this imposes a strong constraint for calculation methods. Finally, the small geometry of some arches allows developing an always stable equilibrium and the ultimate load would be associated with the material failure. It is rather impossible to find such a structural performance for large span arches.

Three calculation methods: funicular limit analysis, kinematic limit analysis and up-to-date two-dimensional finite element method, have been extensively used for large span masonry arches. But when applied to arches with few voussoirs results do not always match. First of all, it is worth noticing that only the finite element method was able to provide results for every analysed case, so it could be presented as the most robust calculus method among the three tested. Classical methods (limit analysis and kinematic analysis) do not usually achieve an ultimate load close enough to the experimental one (with relative errors over 30%). Limit analysis works pretty well for continuous geometries or discrete geometries with a lot of joints because it is easy to fit the thrust line inside the boundaries of the arch and reproduce the hinges. On the contrary, for arches with few voussoirs it is very difficult to set a thrust line with a catenary shape and reproduce the hinges (points with the thrust line tangent to the arch's boundary) at the real joints. Because of the geometry constraint (few voussoirs) it is difficult to full fill the equilibrium and the kinematic mechanism. Therefore, limit analysis without further possible modifications do not reproduce the ultimate load with an acceptable approach for this problem. The kinematic analysis also works better for large number of voussoirs because it is easier to find a boundary-compatible mechanism close to the real one. Although adding fiction joints may be used to apply these two methods in arches with a few voussoirs, this procedure seems not recommendable as real collapse mechanisms will appear always with hinges in the real joints. Voussoirs will not crack by tension so no added joint should be used.

FEA simulations provide the evidence that considering the sliding failure mode is a real need to assess the strength of arches whose failure mode could be partially determined by a sliding process. Furthermore, these simulations have obtained the best fitting with the experimental results among the compared methods and its applicability has been proved to be the widest of the analysed cases. With an average error of 6.8% (Table 5), the finite element analysis seems to be able to correctly predict all the tested cases, whose average scattering is 9.5% (calculated from the tests with more than one repetition: B.1, C.1 and D.1). Finally, it has been observed that the correct definition of contacts is essential to provide accurate results when using finite element methods with this kind of arches.

## References

- Alfano, G and Crisfield, M.A. (2001), "Finite element interface models for the delamination analysis of laminated composites: mechanical and computational issues", *Int. J. Numer. Meth. Eng.*, **50**, 1701-1736.
- Andreu, A., Gil, L. and Roca, P. (2007), "Computational analysis of masonry structures with a funicular model", *J. Eng. Mech.*, **133**(4), 473-480.
- Audenaert, A., Peremars, H. and Reniers, G. (2007), "An analytical model to determine the ultimate load on masonry arch bridges", *J. Eng. Math.*, **59**(3), 323-336.
- Boothby, T.E. (2001), "Load rating of masonry arch bridges", *J. Bridge Eng.*, **6**(2), 79-86.
- Borri, A., Castori, G. and Corradi, M. (2011), "Intrados strengthening of brick masonry arches with composite materials", *Compos. Part. B-Eng.*, **38**(2), 144-151.

- Cavicchi, A. and Gambarotta, L. (2006), "Two-dimensional finite element upper bound limit analysis of masonry bridges", *Comput. Struct.*, **84**(19-20), 2316-2328.
- Chen, Y., Ashour, A.F. and Garrity, S.W. (2007), "Modified four-hinge mechanism analysis for masonry arches strengthened with near surface reinforcement", *Eng. Struct.*, **29**, 1864-1871.
- de Arteaga, I. and Morer, P. (2012), "The effect of geometry on the structural capacity of masonry arch bridges", *Constr. Build. Mater.*, **34**(1), 97-106.
- Drosopoulos, G.A., Stavroulakis, G.E. and Massalas, C.V. (2006), "Limit analysis of a single span masonry bridge with unilateral frictional contact interfaces", *Eng. Struct.*, **28**, 1864-1873.
- Drosopoulos, G.A., Stavroulakis, G.E. and Massalas, C.V. (2008), "Influence of the geometry and the abutments movement on the collapse of stone arch bridges", *Constr. Build. Mater.*, **22**(3), 200-210.
- Fanning, P.J. and Boothby, T.E. (2001), "Three-dimensional modelling and full-scale testing of stone arch bridges", *Comput. Struct.*, **79**(29-30), 2645-2662.
- Garmendia, L., San-José, J.T., García, D. and Larrinaga, P. (2011), "Rehabilitation of masonry arches with compatible advanced composite material", *Constr. Build. Mater.*, **25**(12), 4374-4385.
- Heyman, J. (1997), *The Stone Skeleton: Structural Engineering of Masonry Architecture*, Cambridge Univ. Press, Cambridge.
- Milani, E., Milani, G. and Tralli, A. (2008), "Limit analysis of masonry vaults by means of curved shell finite elements and homogenization", *Int. J. Solids. Struct.*, **45**(20), 5258-5288.
- Roca, P., López-Almansa, F., Miquel, J. and Hanganu, A. (2006), "Limit analysis of reinforced masonry vaults", *Eng. Struct.*, **29**, 431-439.

## Annex

Experimental observations of the tests carried out are detailed in this annex. To analyse the results, voussoirs were numbered from the left to the right side of the sketches in Fig. 1. In the same way, the four theoretical hinges that may develop were labelled from H1 to H4 corresponding with left to right direction in sketches in Fig. 1. The behaviour of each arch during the test is described below:

### *Test A.1.1*

The hinge H1 between the 2<sup>nd</sup> and 3<sup>rd</sup> voussoir was initially open in the extrados because of geometric imperfections of the pieces that constitute the arch. At lower loads (100 N approx.) the hinge H4 between the 9<sup>th</sup> voussoir and the support opened in the intrados. When increasing the load (125 N approx) the hinge H2 appeared opening the intrados of the arch between the 4<sup>th</sup> and 5<sup>th</sup> voussoirs. Continuing with increasing the load, hinges H1 and H4 grew fast. In the case of H1, this hinge position is not clear as it opened joints between basis and 1<sup>st</sup> voussoir, between 1<sup>st</sup> and 2<sup>nd</sup> voussoirs and between 2<sup>nd</sup> and 3<sup>rd</sup> voussoirs. H4 was perfectly located and H2 did not grow from its appearance time. At 250 N approx. the hinge H2 began growing and at 275 N approx. the hinge H3 finally appeared between 7<sup>th</sup> and 8<sup>th</sup> voussoirs but the arch did not collapse yet. When applying 326 N the hinge H3 definitely grew and the arch suddenly collapsed by formation of the mechanism.

### *Test A.2.1*

In this case, the first hinge which appeared was H2 between 4<sup>th</sup> and 5<sup>th</sup> voussoirs. Simultaneously (100 N approx.), H4 appeared between 9<sup>th</sup> voussoir and the basis. At 150 N the hinge H3 opened the extrados of the arch between 7<sup>th</sup> and 8<sup>th</sup> voussoirs. From this point and on all hinges grew up to reach the 301 N when the hinge H1 between 2<sup>nd</sup> and 3<sup>rd</sup> voussoirs appeared and the arch suddenly collapsed.

### *Test B.1.1*

H4 (between 8<sup>th</sup> voussoir and basis) is initially opened because the contact with the support was not regular. It grew during the test. H2 appeared between 3<sup>rd</sup> and 4<sup>th</sup> voussoirs opening the intrados of the arch at 150 N and increased during the test. When applying 300 N the arch geometry changed in a very substantial way. It corresponded with the opening of the hinge H3. The hinge H1 is not appreciable until the arch's sudden collapse when applying 335 N.

### *Test B.1.2*

H4 (between 8<sup>th</sup> voussoir and the base) is initially opened at the intrados. The contact between the 1<sup>st</sup> voussoir and the base is opened at the intrados in contrast with what was expected for hinge H1. In fact, this separation decreased during the test and for approximately 250 N the joint was completely closed. At this point, hinges H2 and H3 suddenly appear and grew up to 20 mm of maximum gap. The arch deformation was significant. At 276 N the arch collapsed when H1 appeared opening the extrados.

### *Test B.2.1*

In contrast with previous B tests, any hinge is initially opened. Hinge H2 was initially distributed

(at 100N) on joints between 3<sup>rd</sup>, 4<sup>th</sup> and 5<sup>th</sup> voussoirs. For 150 N it was clearly located between 4<sup>th</sup> and 5<sup>th</sup> voussoirs. At the same load the hinge H3 appeared opening the extrados between 5<sup>th</sup> and 6<sup>th</sup> voussoirs. At 250 N approx. the joint between the base and 1<sup>st</sup> voussoir opened at the intrados. At 275 N approx. the hinge H4 appeared between the 8<sup>th</sup> voussoir and the base. For 301 N the arch collapsed with far less deformation than the previous two tests on B series. H1 is suddenly formed during the collapse process.

#### *Test C.1.1*

The following joints were opened at the beginning of the test: intrados between the 1<sup>st</sup> voussoir and the base (2mm approx.) and between the 19<sup>th</sup> voussoir and the base (2mm approx., hinge H4), intrados between 8<sup>th</sup> and 9<sup>th</sup> voussoirs (less than 1 mm, hinge H2) and extrados between 15<sup>th</sup> and 16<sup>th</sup> voussoirs, hinge H3. At lower loads, the joints between 19<sup>th</sup>-base and 15<sup>th</sup>-16<sup>th</sup> voussoirs grew. For 80 N important deformations were noticed. The arch moved and settled opening more these two hinges. Now the hinge H3 was displaced to 14<sup>th</sup> and 15<sup>th</sup> voussoirs. The arch failed at applying 95 N. H1 was suddenly formed between 3<sup>rd</sup> and 4<sup>th</sup> voussoirs. Mixed mechanism-contact sliding failure was observed. It was the same joint with hinge H2 the one which slide.

#### *Test C.1.2*

At the beginning of the test joints between 1<sup>st</sup>-base (intrados), 9<sup>th</sup>-10<sup>th</sup> (intrados, H2), 15<sup>th</sup>-16<sup>th</sup> (extrados, H3) and 19<sup>th</sup>-base (intrados, H4) were opened. During the test, hinges H2 and H3 changed their position to 8<sup>th</sup>-9<sup>th</sup> and 14<sup>th</sup>-15<sup>th</sup> respectively whilst H4 grew. It was the appearance of H1 (4<sup>th</sup>-5<sup>th</sup> voussoirs, extrados) at 90N what caused the failure by formation of a mechanism. No sliding was noticed.

#### *Test D.1.1*

All joints were initially closed. The load was increased up to 300 N when the intrados between 3<sup>rd</sup> and 4<sup>th</sup> voussoirs opened. It was hinge H2. At 375 N opened the joint between 7<sup>th</sup> and 8<sup>th</sup> voussoirs at the extrados. It was hinge H3. These two hinges grew up to 423 N when suddenly the two remaining required hinges appeared between basis and adjacent voussoirs.

#### *Test D.1.2*

All joints were initially closed. For 250 N approx. hinge H2 appeared first between 3<sup>rd</sup> and 4<sup>th</sup> voussoirs. Hinge H3 (between 7<sup>th</sup> and 8<sup>th</sup> voussoirs) opened at 300 N approx. At 350 N the arch collapsed but previously the hinge H3 had been placed between 6<sup>th</sup> and 7<sup>th</sup> voussoirs. H1 and H4 were the same than in the previous test.

#### *Test D.1.3*

All joints were initially closed. For 100N approx. hinge H2 appeared first between 3<sup>rd</sup> and 4<sup>th</sup> voussoirs. After this, hinge H1 between the 1<sup>st</sup> voussoir and the base is formed opening the intrados for 200 N. This two hinges grew for loads up to 500 N without the appearance of any other hinge. Finally, at loading 521 N the two remaining hinges suddenly opened between 6<sup>th</sup> and 7<sup>th</sup> voussoirs (H3) and 10<sup>th</sup>-base position (H4)

#### *Test E.1.1*

The joint between 6<sup>th</sup> voussoir and the support was initially opened at the intrados. During the

loading process this joint closed and for 250 N the intrados between 4<sup>th</sup> and 5<sup>th</sup> voussoir was opened (H3) and the extrados between 2<sup>nd</sup> and 3<sup>rd</sup> (H2) also opened. The arch bore the maximum applicable load opening this two hinges. Almost all deformation was recovered when unloading and H2 was completely closed.

#### *Test E.2.1*

As the previous test, the joint between 6<sup>th</sup> voussoir and the support was initially opened at the intrados but it closed and opened hinge H3 between 5<sup>th</sup> and 6<sup>th</sup> voussoirs instead at 300 N approx. No other hinge is formed at loading the arch up to the maximum experimentally possible for the chosen test setup.

#### *Test E.3.1*

The joint between 6<sup>th</sup> voussoir and the support was initially opened at the intrados. No other hinge appeared when loading up to 200 N but the 6<sup>th</sup> voussoir clearly descended in this case. For 200 N load the hinge H1 between the 1<sup>st</sup> voussoir-base appeared. The hinge H2 was not noticed in all test. Arch did not fail with the applied load.

#### *Test E.4.1*

The load was applied at the extrados of the arch near the contact between the 6<sup>th</sup> voussoir and the support. When beginning the test, hinges H1 (1<sup>st</sup> voussoir-base) and H3 (6<sup>th</sup> voussoir-support) were opened at the intrados. They grew during the test and for 175 N, H2 (extrados 3<sup>rd</sup>-4<sup>th</sup> voussoirs) appeared. At reaching 206 N the arch failed by a mechanism which included the glide of 6<sup>th</sup> voussoir respect the support.

#### *Test E.5.1*

Hinge H3 (6<sup>th</sup> voussoir - support, intrados) was initially observed. At 150 N hinge H1 (1<sup>st</sup> voussoir-base, intrados) appeared. At 175 N the arch has deformed noticeably and hinge H2 (3<sup>rd</sup>-4<sup>th</sup> voussoirs extrados) had appeared. However the arch bore up to 196 N.

#### *Test E.6.1*

Only the hinge H1 (1<sup>st</sup> voussoir-base, intrados) was initially formed before loading. When 200 N applied the hinge H3 (6<sup>th</sup> voussoir-support) appeared at the intrados. At 221 N the hinge H2 appeared between 3<sup>rd</sup> and 4<sup>th</sup> voussoirs and the arch failed suddenly with less previous deformation than in the cases E.4.1 and E.5.1.

#### *Test F.1.1*

The load was applied at 7<sup>th</sup> voussoir. The contact between 10<sup>th</sup> voussoir and support was initially opened at the extrados. This hinge did not grow when loading 50 N but hinge H1 appeared opening the intrados between the 1<sup>st</sup> voussoir and the base. The intrados between 7<sup>th</sup> and 8<sup>th</sup> voussoirs opened at 95 N. It was hinge H3. The rotation of the hinges at 7<sup>th</sup>-8<sup>th</sup> and 10<sup>th</sup>-support increased during the load up to 150 N. When reaching 200 N the last hinged required appeared (extrados 3<sup>rd</sup>-4<sup>th</sup> voussoirs, H2) but the arch did not collapsed. The failure happened at loading 275 N.

#### *Test F.2.1*

The load was applied at 9<sup>th</sup> voussoir, near vertical support. The 1<sup>st</sup> voussoir-base contact was initially

opened at the intrados forming hinge H1. Loading 30 N the second hinge, H2, appeared at the extrados between 4<sup>th</sup> and 5<sup>th</sup> voussoirs. Applying 40 N the extrados of the contact of the 10<sup>th</sup> voussoir with the support opened at the same time this voussoir glide down a noticeable distance (about 5 mm). When applying 49 N the contact between 10<sup>th</sup> voussoir and the support changed and the intrados was opened forming the hinge H3. At the same time, hinge H1 changed its position and opened the intrados between 1<sup>st</sup> and 2<sup>nd</sup> voussoirs. At this load the arch failed. A mixed sliding and mechanism failure modes was observed.